TECHNOLOGICAL UNIVERSITY DELFT

DEPARTMENT OF AERONAUTICAL ENGINEERING

Report VTH-124

THEORETICAL AND EXPERIMENTAL INVESTIGATIONS OF INCOMPRESSIBLE LAMINAR BOUNDARY LAYERS WITH AND WITHOUT SUCTION

Ph.D THESIS

J.L. van INGEN

DELFT
the NETHERLANDS

OCTOBER, 1965

This PDF-file contains chapter 6:

Phase plane description of the boundary layer flow between non-parallel plane walls

6. Phaseplane description of the boundary-layer flow between non-parallel plane walls.

6.1. Introductory remarks.

From the examples discussed in chapter 5 it follows that the behaviour of boundary-layer flows strongly depends on the streamwise pressure gradient and the suction velocity.

Another important example which may illustrate this is the viscous flow between non-parallel plane walls. This flow has been discussed already in 1915 and 1916 by Jeffery [23] and Hamel [24] respectively using the Navier-Stokes equations. From their work it is known that in the case of inflow between non-porous walls the Navier-Stokes equations admit a boundary layer type solution for which the radial velocity component becomes practically constant at large distances from the wall.

For inflow between impervious walls such a boundary layer type solution is also allowed by the boundary layer equations. This solution was given in closed form by Pohlhausen in 1921 [22]; it will be discussed further in section 6.3.

For outflow between diverging walls it is only possible to obtain boundary layer type solutions in case a sufficient amount of suction at the wall is applied.

This characteristic difference between the cases of inflow and outflow becomes very clear when the flow is studied in a "phase plane" where shear τ is plotted versus the velocity component u parallel to the wall.

The phase plane concept is known from the theory of oscillations of non-linear autonomous systems with one degree of freedom where speed is plotted versus displacement. These oscillations are described by a second order ordinary differential equation in the variables displacement x and time t of the form

$$\frac{d^2x}{dt^2} + g(x, \frac{dx}{dt}) = 0 \qquad (6.1)$$

As the time t does not appear explicitly in this equation it can be eliminated between (6.1) and

$$y = \frac{dx}{dt} \tag{6.2}$$

where y denotes the speed.

The resulting equation is of the form

$$\frac{dy}{dx} = \frac{P(x,y)}{Q(x,y)} \tag{6.3}$$

Singular points of this equation occur for values of x and y where both P and Q vanish; the singular points correspond to equilibrium positions of the oscillation. The type of singularity determines the character of the stability (or instability) of the oscillation.

A general theory of equation (6.3) has been given by Poincaré [68]; reviews of this theory may be found for instance in the books by Minorsky [69] and Stoker [70].

If the origin of a Cartesian coordinate system coincides with the singular point under investigation equation (6.3) may be written in the form

$$\frac{dy}{dx} = \frac{ax + by + P_1(x,y)}{cx + dy + Q_1(x,y)} \tag{6.4}$$

where $P_1(o,o) = Q_1(o,o) = 0$. If P_1 and Q_1 vanish like x^2+y^2 when x and y tend to zero and if furthermore $ad - bc \neq 0$ the type of singularity is determined by the simpler equation

$$\frac{dy}{dx} = \frac{ax + by}{cx + dy} \tag{6.5}$$

A classification of the singularities may then be given in terms of the constants a, b, c and d (see for instance Stoker [70]) and hence the different kinds of singularities of (6.3) may be determined without actually solving the equation.

In the following section it will be shown that for the flow between non-parallel plane walls the boundary layer equations can be reduced to the form (6.1) so that the phase plane method may be used to study the flow problem. It follows also that the singular points correspond to the edge of the boundary layer; solutions of the boundary layer type will only occur when the singularity is a saddle point or a stable node. The kind of

singularity will depend on the amount of suction or blowing; it is found for instance that for outflow between diverging walls a minimum amount of suction has to be exceeded before a boundary layer type solution will be possible.

A similar treatment may be given for the full Navier-Stokes equations; the results are essentially the same as for the boundary layer equations. In some cases it is even possible to transform the Navier-Stokes equations into the boundary-layer equations by introducing suitable new variables; only the boundary conditions remain different. This difference in boundary conditions vanishes when the Reynoldsnumber becomes large and the solutions of the Navier-Stokes equations then tend to those of the boundary layer equations. In this thesis only the results for the boundary layer equations will be given. A more detailed review of this work, together with the phase plane description applied to the Navier-Stokes equations, may be found in [71].

As far as the author is aware, the only other phase plane representation of viscous flow has been given by Ku [72] who discussed the boundary layer flow for the flat plate and the plane stagnation point. As the equations (3.14) and (3.20) describing these flows are of the third order a phase space is needed instead of a phase plane. Since the general theory for singularities in a three dimensional space is more complicated than for the two-dimensional problem, Ku was unable to establish a relation between the types of singularities and the character of the flow.

6.2. The boundary layer equations for the flow between non-parallel plane walls.

For radial flow between non-parallel plane walls (fig. 6.1) the potential flow velocity distribution is given by

$$U = u_1 x^{-1} \tag{6.6}$$

where u_1 is a constant. For $u_1 > 0$ equation (6.6) represents outflow from a two-dimensional source at $x = 0$; for $u_1 < 0$ inflow into a sink is obtained. It has been mentioned already in section 3.1.1 that for $U = u_1 x^{-1}$ the boundary layer equation (2.7) and the continuity equation (2.5) admit a similar solution. To obtain this solution the non-dimensional

wall distance η is introduced with

$$\eta = \frac{y}{x}\sqrt{\frac{|u_1|}{\nu}} \tag{6.7}$$

and the non-dimensional streamfunction $f(\eta)$ by

$$\psi = \sqrt{\nu\,|u_1|}\; f(\eta) - \lambda\sqrt{\nu|u_1|}\; \ell n\, x \tag{6.8}$$

In equation (6.8) λ is a constant which determines the suction velocity at the wall according to equation 6.15.
With (3.7) and (6.8) the continuity equation (2.5) is satisfied; the velocity components u and v follow from

$$u = \frac{|u_1|}{x}\, f'(\eta) = |U|\, f'(\eta) \quad \text{or} \quad \bar{u} = \frac{u}{|U|} = f'(\eta) \tag{6.9}$$

$$v = \sqrt{\nu|u_1|}\,\frac{\eta}{x}\, f'(\eta) + \frac{\lambda}{x}\sqrt{\nu|u_1|} \tag{6.10}$$

In (6.9), (6.10) and subsequent equations in this chapter primes denote differentiation with respect to η.
Introduction of (6.9) and (6.10) in the boundary layer equation (2.7) leads to

$$f''' - \lambda f'' + (f')^2 - 1 = 0 \tag{6.11}$$

Since f does not occur in (6.11) the order of this equation may be reduced through the introduction of $f' = \bar{u}$. The resulting equation is

$$\bar{u}'' - \lambda \bar{u}' + \bar{u}^2 - 1 = 0 \tag{6.12}$$

Boundary conditions for solutions of (6.12) are at the wall

$$\eta = 0 : \bar{u} = 0 \tag{6.13}$$

and at the edge of the boundary layer $\eta \to \infty$:

$$\left.\begin{aligned} &\bar{u} \to +1 \quad \text{for outflow} \quad (u_1 > 0) \\ &\bar{u} \to -1 \quad \text{for inflow} \quad (u_1 < 0) \\ &\bar{u}' \to 0 \quad \text{both for outflow and inflow} \end{aligned}\right\} \tag{6.14}$$

It follows from (6.10) that the normal velocity at the wall ($\eta = 0$) is given by

$$v_o = \frac{\lambda}{x}\sqrt{\nu\,|u_1|} \tag{6.15}$$

This equation shows that v_o should be inversely proportional to x to obtain similar solutions; blowing occurs for $\lambda > 0$ and suction for $\lambda < 0$.

6.3. The non-porous wall ($\lambda = 0$).

For the non-porous wall ($\lambda = 0$) equation (6.12) can easily be integrated after multiplication with $2\,\bar{u}'$. The result is

$$(\bar{u}')^2 + \frac{2}{3}\bar{u}^3 - 2\,\bar{u} = A \tag{6.16}$$

where A is an integration constant.

For inflow the boundary conditions (6.14) at the edge of the boundary layer require that $A = +\frac{4}{3}$. Then it follows from (6.16) that at the wall $(\bar{u}')^2 = \frac{4}{3}$; hence the non-dimensional shear stress at the wall is given by $\bar{u}'(o) = -2/\sqrt{3}$. The negative root is taken because in the present coordinate system both the velocity and shear stress are negative for the case of inflow.

For outflow the conditions (6.14) at the edge of the boundary layer lead to $A = -\frac{4}{3}$. However, from (6.16) it follows that A should be non-negative to obtain a real value for the skin friction at the wall ($\bar{u} = 0$). Hence it is concluded that (6.16) does not allow a real boundary layer type solution for outflow.

The solution for inflow with $A = +\frac{4}{3}$ can be written in the forms

$$\frac{d\bar{u}}{d\eta} = \bar{u}' = -\sqrt{\frac{4}{3} + 2\,\bar{u} - \frac{2}{3}(\bar{u})^3} \tag{6.17}$$

$$\eta = -\int_o^{\bar{u}} \frac{d\bar{u}}{\sqrt{\frac{4}{3} + 2\,\bar{u} - \frac{2}{3}\bar{u}^3}} \tag{6.18}$$

Again the minus-signs in (6.17) and (6.18) are introduced since for the case of inflow both $\bar{u}$ and $\bar{u}'$ are negative. Integration of (6.18) leads to the following expression for the velocity profile

$$-\bar{u} = 3\ \mathrm{tgh}^2 \left[\frac{\eta}{\sqrt{2}} + 1.146\right] - 2 \qquad (6.19)$$

A graph of the velocity profile is shown in fig. 6.2. The solution (6.19) was obtained by Pohlhausen in 1921 [22]. (see also [7], chapter 9.b).

That a corresponding solution for outflow does not exist can easily be demonstrated by studying equation (6.12) in the phase plane. Introducing the non-dimensional shear stress $\bar{\tau}$ by

$$\bar{\tau} = \bar{u}' = \frac{d\bar{u}}{d\eta} \qquad (6.20)$$

equation (6.12) may be written, for $\lambda = 0$, in the form

$$\frac{d\bar{\tau}}{d\eta} = 1 - \bar{u}^2 \qquad (6.21)$$

Elimination of η between (6.20) and (6.21) leads to the following first order differential equation

$$\frac{d\bar{\tau}}{d\bar{u}} = \frac{1-\bar{u}^2}{\bar{\tau}} \qquad (6.22)$$

Since equation (6.22) is of the form (6.3) it can easily be studied using Poincaré's general theory. Singular points are obtained for $\bar{\tau} = 0$ and $\bar{u} = -1$ or $+1$; these points in the phase plane correspond to the edge of the boundary layer in the physical plane for inflow and outflow respectively. Solutions of (6.22) are easily found to be

$$\bar{\tau}^2 = 2\,\bar{u} - \frac{2}{3}\,\bar{u}^3 + A \qquad (6.23)$$

where A is an arbitrary integration constant. Integral curves for different values of A are shown in fig. 6.3. These trajectories were obtained by solving (6.12) on an analog computer for different initial

conditions; the curves in fig. 6.3 were drawn by a plotting machine coupled to the analog computer. Arrows in fig. 6.3 indicate the direction in which the trajectories are traversed with increasing wall distance η. This direction follows from (6.20) which shows that η increases with $\bar{u}$ when $\bar{\tau}$ is positive.

The singularity at (-1,0) in the phase-plane is a saddle point; it corresponds to the edge of the boundary layer for inflow. At (+1,0) a center occurs which represents the edge of the boundary layer for outflow.

A solution of (6.22) which satisfies the boundary conditions (6.13) and (6.14) should produce a trajectory in the phaseplane connecting a point on the $\bar{\tau}$-axis ($\eta = \bar{u} = 0$) with one of the singularities. It follows from fig. 6.3 that such a solution may be found for inflow; it is defined by the trajectory PS for which $A = +\frac{4}{3}$. This trajectory clearly represents Pohlhausen's solution (6.17).

The boundary layer velocity profile follows from

$$\eta = \int_0^{\bar{u}} \frac{d\bar{u}}{\bar{\tau}} \qquad (6.24)$$

it can easily be produced by the analog computer. The velocity profile obtained in this way is shown in fig. 6.4 together with the profiles corresponding to some adjacent trajectories in fig. 6.3. The figure shows that Pohlhausen's solution is a unique one. It should also be noted that the solutions of (6.22) for the case of inflow show the same behaviour as the Hartree solutions for the Falkner-Skan equation in case $\beta > 0$ (cf. section 3.1.2).

It is clear from fig. 6.3 that no boundary layer type solution can be found for outflow because (+1,0) is an isolated singular point. It will be shown in the next section that for outflow boundary layer type solutions may be found only if a sufficient amount of suction is applied at the wall.

6.4. The effects of suction and blowing ($\lambda \neq 0$).

For $\lambda \neq 0$ the walls of the channel should be porous giving a normal

velocity distribution in accordance with equation 6.15. This equation shows that there is suction at one wall and blowing at the other one with a normal velocity inversely proportional to x. In what follows only the lower wall will be considered for which $\lambda < 0$ or $\lambda > 0$ means suction or blowing respectively. A solution of (6.12) in closed form can not be found for $\lambda \neq 0$. According to Mangler [37] numerical solutions have been obtained by Holstein [73]; detailed numerical results will not be given in the present work however. Instead of this, equation (6.12) will be studied in the phase plane giving a better insight into the structure of the equation.

Introducing $\bar{\tau} = \frac{d\bar{u}}{d\eta}$ and eliminating η from (6.20) and (6.12) leads to the following equation

$$\frac{d\bar{\tau}}{d\bar{u}} = \frac{\lambda\bar{\tau} + 1 - \bar{u}^2}{\bar{\tau}} \qquad (6.25)$$

Equation (6.25) is again of the type (6.3) and hence can easily be studied using Poincaré's theory. For all values of λ the singular points are found at $\bar{\tau} = 0$, $\bar{u} = \pm 1$ and hence are the same as in the no-suction case ($\lambda = 0$). It is easily found that the singular point (-1,0), representing the edge of the boundary layer for inflow, is always a saddle point irrespective of the amount of suction or blowing. The type of the singularity at (+1,0), corresponding to the edge of the boundary layer for outflow, depends on the value of λ according to table 6.1.

Phase plane portraits for different values of λ, obtained from the analog computer, are shown in fig. 6.5.

Since the singularity at (-1,0) is always a saddle point there is a unique boundary layer type solution for the case of inflow irrespective of the amount of suction or blowing. These solutions correspond to the trajectories connecting the $-\bar{\tau}$ axis with the singularity (-1,0). The corresponding velocity profiles are shown in fig. 6.6 for different values of λ.

A boundary layer type solution for outflow would require a trajectory in the phase plane connecting some point on the $+\bar{\tau}$-axis with the singularity (+1,0). Fig. 6.5 shows that for blowing ($\lambda > 0$) all trajectories lead

away from the singular point. Hence, a boundary layer type solution is not possible for outflow with blowing at the wall. From section 6.3 it is known already that also for the impervious wall ($\lambda = 0$) no solution is possible.

For suction at the wall ($\lambda < 0$) an infinity of solutions exists; however not all these solutions are physically acceptable. For $-2\sqrt{2} < \lambda < 0$ the singularity at (+1,0) is a spiral point which produces velocity profiles of the type shown in fig. 6.7. In this case $\bar{u}$ approaches 1 in an oscillatory manner which is physically not acceptable. With increasing intensity of suction the spiral changes into a stable node for $\lambda \leq -2\sqrt{2}$; the corresponding velocity profiles are of the type shown in fig. 6.8. Some of the velocity profiles have an overshoot and hence are rejected as physically unacceptable. There remains however an infinity of solutions for which $\bar{u} \longrightarrow 1$ from below; it is not clear on physical grounds which of these solutions should be selected as the relevant one. This situation is analogous to the problem encountered by Hartree in his study of solutions of the Falkner-Skan equation (3.10) for $\beta < 0$ (see section 3.1.2). To obtain a unique solution Hartree introduced the extra condition that the relevant solution is the one for which $\bar{u} \longrightarrow 1$ as fast as possible without making an overshoot. If this "Hartree condition" is also accepted for the present problem it follows that the steeper main branch of the stable node should be used (fig. 6.9). Some further arguments in favour of Hartree's choice can be produced in the present case. If it is required that $\bar{u}$ approaches 1 exponentially it should be possible to develop $\bar{\tau}$ in a power series in $(\bar{u}-1)$ starting with a term of the first degree. This is only possible for the two main branches of the node; the other trajectories through the node can only be represented by non-analytical series. The power series for the steeper main branch has finite coefficients for all values of $\lambda \leq -2\sqrt{2}$; for the other main branch however some of the coefficients in the series may become infinite at certain values of λ. Hence if $\bar{u}$ should tend to 1 exponentially with η for all values of λ, only the steeper main branch of the node may be used; this is in agreement with Hartree's choice.

A further argument follows from an inspection of the phase plane portraits in fig. 6.5. It follows that with increasing suction the steeper main

branch moves into a region with higher shear and hence produces a thinner boundary layer. For the other main branch, however, increased suction produces a smaller values of $\bar{\tau}$ and a thicker boundary layer; this conflicts with our physical ideas about the effects of suction on boundary layer flows.

If, finally, the steeper main branch of the node is selected as representing the relevant boundary layer type solution for the case of outflow a unique velocity profile is obtained for $\lambda \leqslant -2\sqrt{2}$. The velocity profiles for some values of λ are shown in fig. 6.6.

From fig. 6.5 it follows that for $\lambda \longrightarrow -\infty$ the wall shear stress becomes very high and the steeper main branch of the node tends to a straight line through (+1,0). In the same way the relevant trajectory through the saddle point becomes a straight line. This property is shown more clearly after introduction of the following transformations

$$\eta_1 = -\lambda \eta \tag{6.26}$$

$$\bar{\tau}_1 = \frac{\bar{\tau}}{-\lambda} = \frac{d\bar{u}}{d\eta_1} \tag{6.27}$$

Substituting (6.26) and (6.27) into (6.25) leads to the following equation

$$\frac{d\bar{\tau}_1}{d\bar{u}} = \frac{-\bar{\tau}_1 + \frac{1-\bar{u}^2}{\lambda^2}}{\bar{\tau}_1} \tag{6.28}$$

which for $\lambda \longrightarrow -\infty$ reduces to

$$\frac{d\bar{\tau}_1}{d\bar{u}} = -1 \tag{6.29}$$

From (6.29) it follows that the trajectories through the singularities $(\pm 1,0)$ are given by

$$\bar{\tau}_1 = 1 - \bar{u} \quad \text{for outflow} \tag{6.30}$$

$$\bar{\tau}_1 = -1 - \bar{u} \quad \text{for inflow} \tag{6.31}$$

Using (6.26), (6.27) and integrating (6.30) and (6.31) leads to

$$\left|\bar{u}\right| = 1 - e^{-\eta_1} = 1 - e^{\lambda \eta} \tag{6.32}$$

With (6.7) and (6.15) equation (6.32) may be written in the form

$$\left|\bar{u}\right| = 1 - e^{\frac{v_o y}{\nu}} \tag{6.33}$$

Equation (6.33) shows that both for outflow and for inflow with increasing suction the velocity profile tends to the asymptotic suction profile discussed in section 3.1.5. This result had been obtained already by Pretsch [74] (see Mangler [37]).

6.5. Consequences of some results of the phase plane description for practical boundary layer calculations.

For the case of inflow between impervious walls equation (6.17) shows that the relation between $\bar{\tau}^2$ and $\bar{u}$ is given by the following polynomial

$$\bar{\tau}^2 = -\frac{2}{3}\,\bar{u}^3 + 2\,\bar{u} + \frac{4}{3} \tag{6.34}$$

or

$$\bar{\tau}^2 = \frac{2}{3}\,(\bar{u}+1)^2(2-\bar{u}) \tag{6.35}$$

In the last part of section 6.4 it was shown that both for outflow and for inflow the asymptotic suction profile is obtained when $\lambda \longrightarrow -\infty$. From equations (6.30) and (6.31) it follows that also in these cases the relation between $\bar{\tau}_1^2$ and $\bar{u}$ is a simple polynomial.
It can be shown that for the case of inflow, at arbitrary values of λ, $\bar{\tau}$ may be developed in a power series in $(\bar{u}+1)$ of the form

$$\bar{\tau} = \gamma_1(\bar{u}+1) + \gamma_2\,(\bar{u}+1)^2 + \gamma_3(\bar{u}+1)^3 + \ldots\ldots \tag{6.36}$$

(note that for inflow $\bar{u} = -1$ at the singularity). It may be shown that the series converges rapidly for all values of λ. For $\lambda = 0$ the

series expansion of $\sqrt{\frac{2}{3}(\bar{u}+1)^2(2-\bar{u})}$ is obtained.
For the case of outflow with $\lambda \leqslant -2\sqrt{2}$ a series expansion around $\bar{u} = +1$ is possible of the form

$$\bar{\tau} = \gamma_1(1-\bar{u}) + \gamma_2(1-\bar{u})^2 + \gamma_3(1-\bar{u})^3 + \ldots. \qquad (6.37)$$

It is found that the series converges well except for values of λ near the limiting value $-2\sqrt{2}$.

The numerical results quoted above suggest the idea that a practical calculation method of the Pohlhausen type can be developed in which the velocity profile is defined by a polynomial expression of the form

$$\bar{\tau}^2 = a_o + a_1\bar{u} + a_2\bar{u}^2 + \ldots\ldots \qquad (6.38)$$

Such a method will be described in the next chapter.

Table 6.1: Type of the singularity for equation (6.25) at (+1,0)

λ	type of singularity
$\leq -2\sqrt{2}$	stable node
$-2\sqrt{2} < \lambda < 0$	stable spiral
0	center
$0 < \lambda < 2\sqrt{2}$	unstable spiral
$\geq 2\sqrt{2}$	unstable node

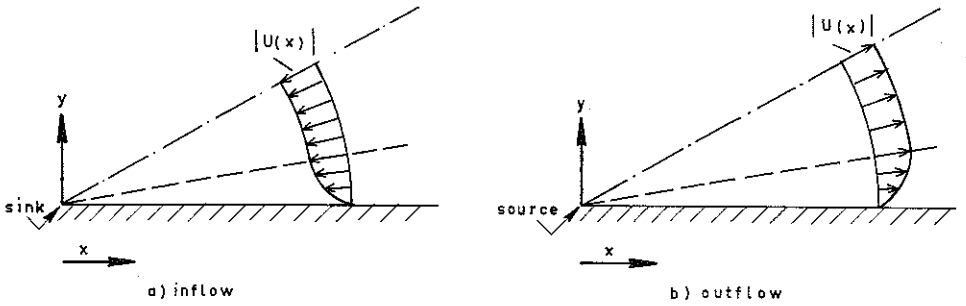

FIG. 6.1: THE FLOW BETWEEN NON-PARALLEL PLANE WALLS.

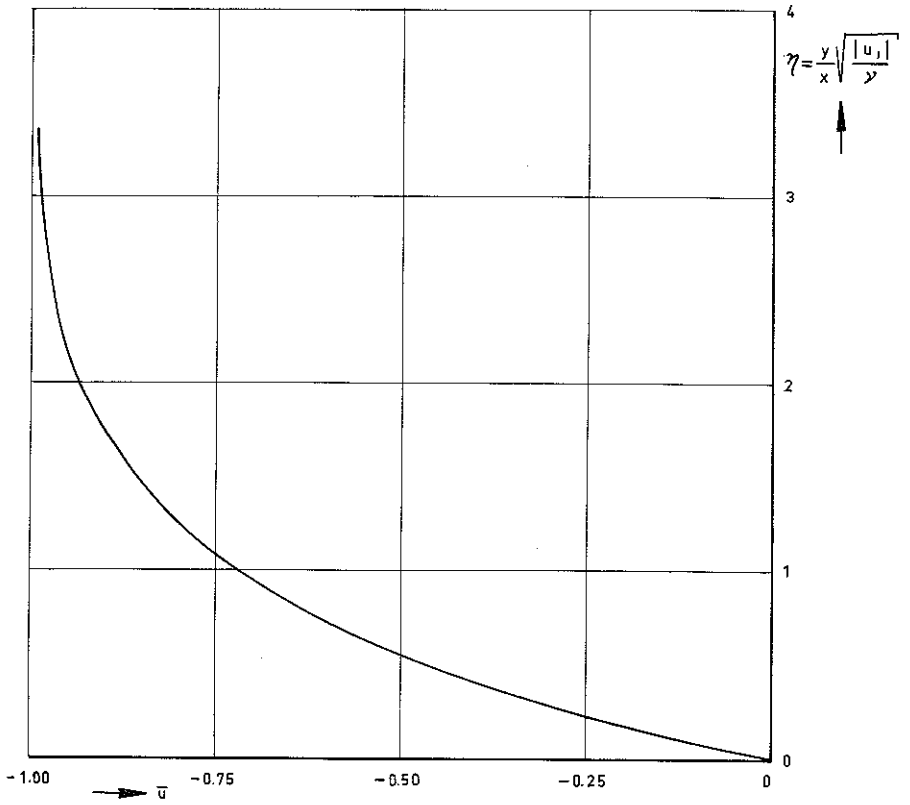

FIG. 6.2: VELOCITY PROFILE FOR INFLOW BETWEEN IMPERVIOUS WALLS (eq.6.19)

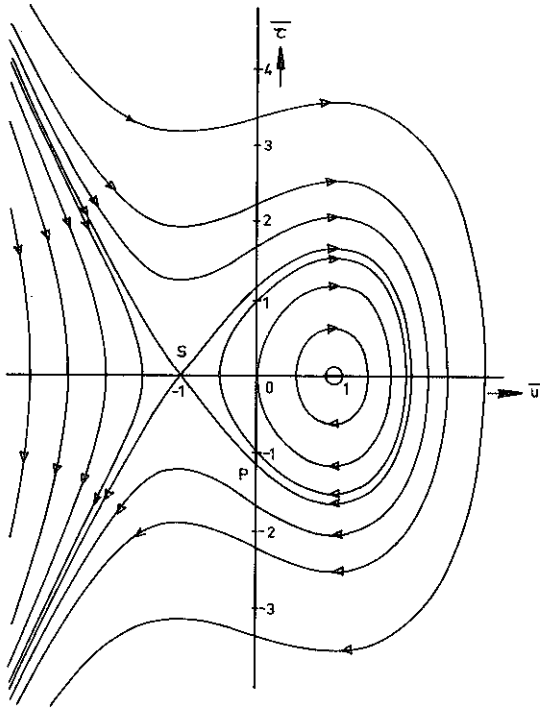

FIG. 6.3: PHASE PLANE PORTRAIT FOR THE BOUNDARY LAYER FLOW BETWEEN IMPERVIOUS NON-PARALLEL PLANE WALLS ($\lambda = 0$)

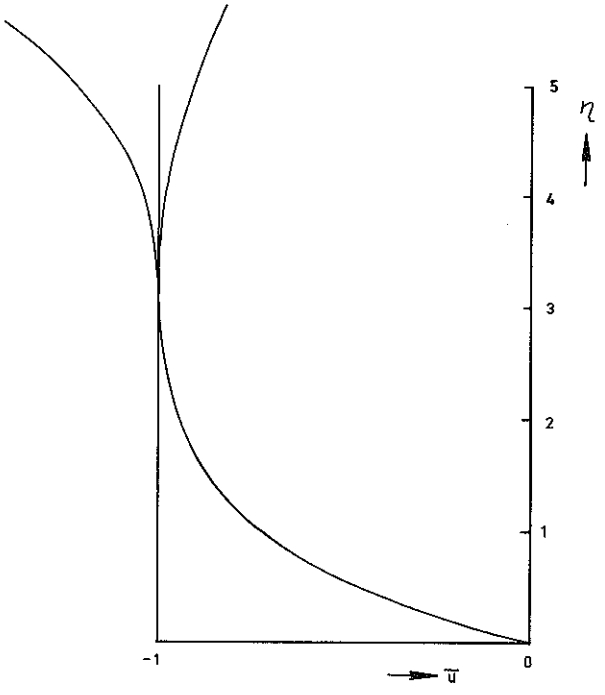

FIG. 6.4: VELOCITY PROFILES CORRESPONDING TO THE SADDLE POINT (−1,0) FOR $\lambda = 0$.

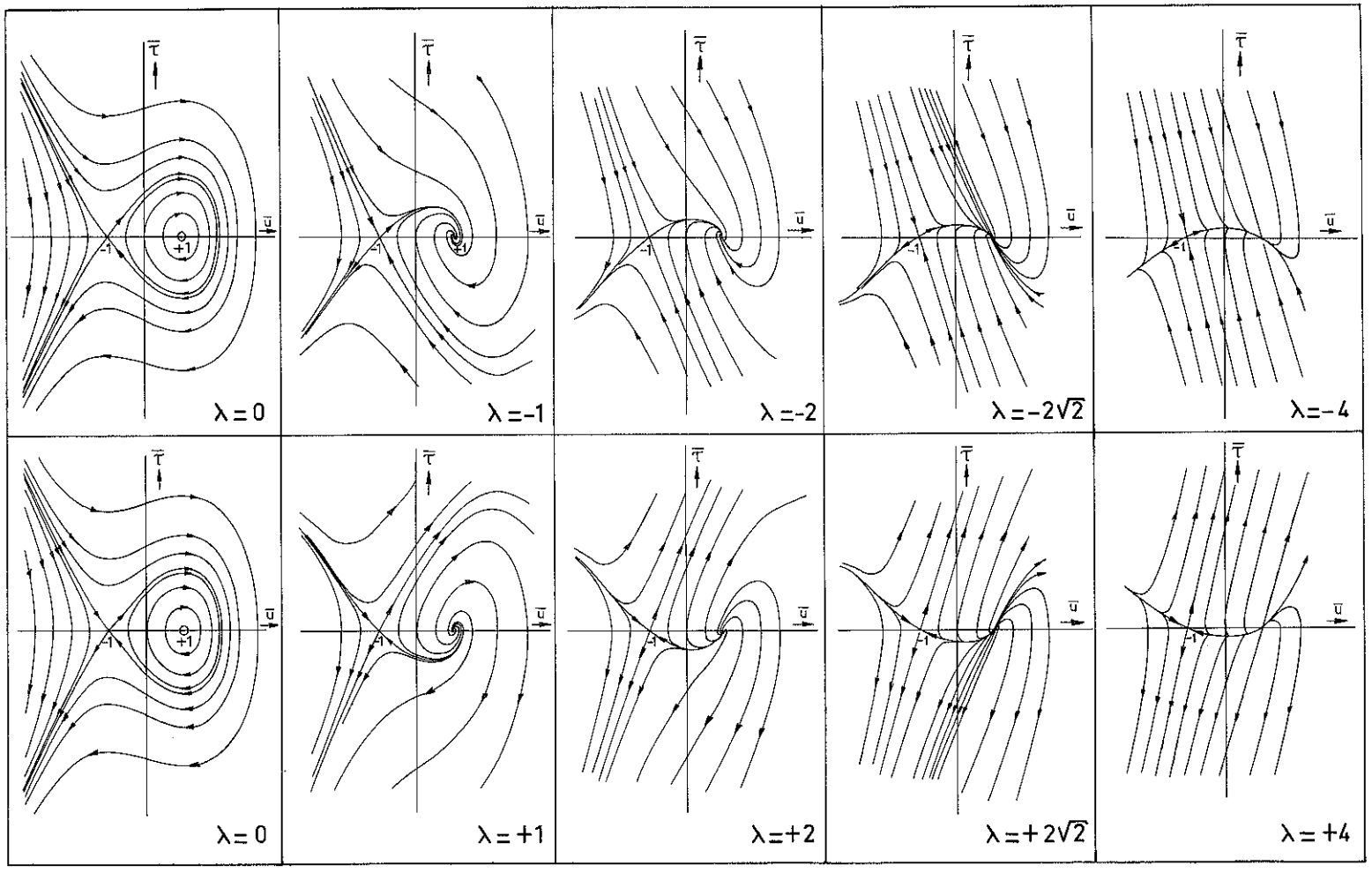

FIG. 6.5: PHASE PLANE PORTRAITS FOR THE BOUNDARY LAYER FLOW BETWEEN POROUS WALLS.

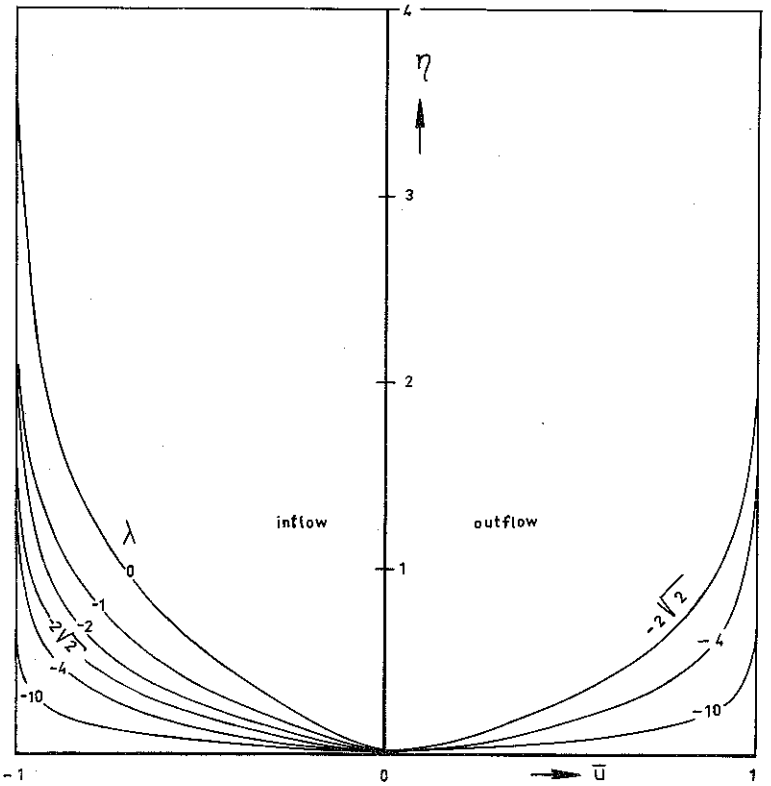

FIG. 6.6: VELOCITY PROFILES FOR INFLOW AND OUTFLOW AT DIFFERENT VALUES OF λ.

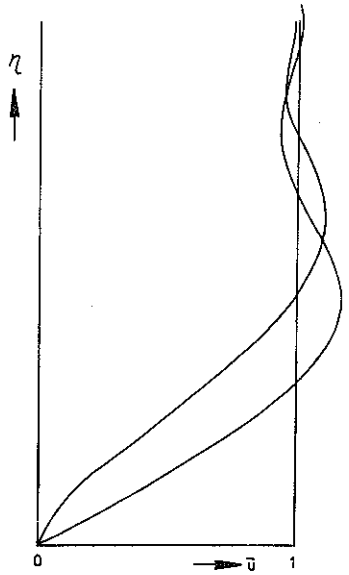

FIG. 6.7: VELOCITY PROFILES FOR OUTFLOW CORRESPONDING TO A STABLE SPIRAL IN THE PHASE PLANE

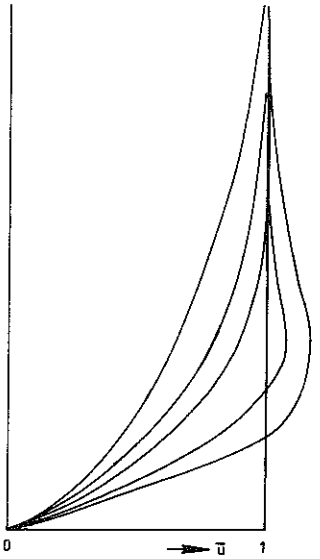

FIG. 6.8: VELOCITY PROFILES FOR OUTFLOW CORRESPONDING TO A STABLE NODE IN THE PHASE PLANE.

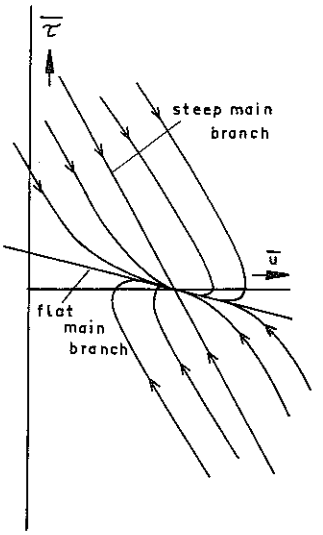

FIG. 6.9: CHARACTERISTICS OF A STABLE NODE.